Fibers and Polymers 2015, Vol.16, No.1, 188-195
DOI 10.1007/s12221-015-0188-5

ISSN 1229-9197 (print version)
ISSN 1875-0052 (electronic version)

Effect of Alumina Nanoparticles on the Enhancement of Impact and Flexural Properties of the Short Glass/Carbon Fiber Reinforced Epoxy Based Composites

Akash Mohanty* and V. K. Srivastava

Department of Mechanical Engineering, Indian Institute of Technology, Banaras Hindu University, Varanasi 221005, India
(Received January 14, 2014; Revised September 13, 2014; Accepted September 21, 2014)

Abstract: Nano scale dispersion due to the size transformation of the reinforced particles from micron size to nano size in the polymer matrix to enhance the mechanical properties of fiber-reinforced hybrid composite is an interesting research topic of the current time. In this study, the nanocomposites test coupons were prepared through the open molding route. The nano scale dispersion is achieved at an optimum concentration of alumina particles (2 wt%), which results in improved thermal stability, impact strength, flexural modulus and flexural strength of composites. The maximum enhancement in impact energy was observed to be 84 % correspond to the addition of 2 wt%, 20 % for the flexural strength correspond to the addition of 3 wt% and 35 % for the flexural modulus correspond to the addition of 5 wt% alumina particles to the epoxy matrix. For the addition of 5 wt% of short glass/carbon fibers to the epoxy, an improvement of 130 % and 170 % for the flexural strength and 55 % and 95 % for the flexural modulus was observed. Furthermore, addition of optimum concentration (i.e. 2 wt%) of alumina nano particle to the 5 wt% glass/carbon fiber reinforced hybrid composites resulted in the improvement of impact properties, flexural strength and flexural modulus of 175 %, 195 %; 18 %, 26 % and 65 %, 85 % as compared to the neat epoxy, and 7 %, 8 %; 82 %, 105 % and 17 %, 5 % as compared to the short fiber reinforced composites. These enhancements in the mechanical properties are mainly due to the better stress transfer properties from fiber and nanoparticle to the matrix, due to the existence of strong interfacial interactions between both epoxy/alumina nanoparticles, which depict the higher resistance to fiber pull out as compare to fiber reinforced composites without alumina nanoparticles.

Keywords: Polymer-matrix composites, Impact strength, Flexural strength, Alumina nano particles, Mechanical testing

Introduction

Particulate and fiber reinforced polymer-matrix composites (PMCs) have been extensively used in many automotive and aeronautical structural applications due to their unique mechanical properties and easiness to produce the tailor-made properties [1,2]. In these types of composites, the thermoset epoxy resins are widely used as a matrix due to many advantages such as easy fabricability, low manufacturing cost, low shrinkage, greater chemical resistance, simple tooling and good adhesion properties [3-6]. Although there are many advantages associated with the composite material like high tensile and impact properties, but the impact behavior of the composite structures is unpredictable which strongly influence the residual load bearing capability [7]. The damage to the composite structures resulted from accidental impacts and classified according to the low/high impact velocity. Low velocity impacts are especially dangerous because it is difficult to detect the damage that may cause reductions in the mechanical properties [8]. During the operational life of composite structural elements or during assembly and maintenance operations, dynamic and impact load applied over it. These loadings originate damage that causes important changes in the behavior of the structural component, and are the main factors that limit the use of the composite materials [9].

It was observed that, some of the structural elements, such as aircraft wings, helicopter blades, mechanical arms, maybe considered as the beam subjected to load that leads to bending moments. Therefore, for the safe design of these components, it is necessary to know the behaviour of the composites when they are subjected to bending moments [10].

To overcome the limitations, lot of attention was focused on nanoparticles for their utilization in traditional composites, as nanoparticles owing to their superior properties emerge as a potential alternatives for reinforcement. The nanoparticles mostly used were alumina nanoparticles [1,11], carbon nanotubes, nanosilica [12-16], clay, as rigid reinforcements in epoxy matrix for various engineering applications. The main advantage of nanocomposites over micro-composites lies in the performance improvement that often acquired at a relatively low concentration of nanoparticles [17]. The clay concentration of 3-5 wt% shows significant improvement in the mechanical properties of the epoxy nanocomposites [16, 18], while single-walled carbon nano tubes (SWCNT) required much lower concentration, i.e., 0.5 wt% to achieve the similar improvement in mechanical properties [19]. Thus, particle size and shape such as spherical, cylindrical, platelet, etc., in relation to the aspect ratio plays an important role in the mechanical performance of the nanocomposites. The remarkable improvement in mechanical properties of nanocomposites was due to the availability of much larger surface-to-volume ratio with a higher percentage of particles atomic surfaces interacting with the matrix (known as surface interaction) [13]. However, at higher concentration of nanoparticles in nanocomposite shows agglomeration, and induce crack propagation owing to the stress concentration

*Corresponding author: mohanty_akash@yahoo.com

[20-24]. In addition, the functionalization of carbon nanotubes further improves the flexural modulus and flexural strength by the addition of very low amount (0.05 wt%) of nanotubes in the epoxy matrix [23]. Impact properties of the nanocomposite improve due to the incorporation of the carbon nanotubes in the epoxy matrix [25]. The addition of montmorillonite (MMT) silicate in glass-fiber-epoxy laminated composites improve the low-velocity impact properties of composite materials [26]. Thus, incorporation of nanoparticles in conventional fiber-reinforced composites improves the mechanical properties.

The main objective of this study is to improve the flexural and impact properties by incorporating alumina nanoparticles along with the glass fibers and carbon fibers into the epoxy matrix. In-situ reduction strategy was used for converting micron size alumina particles into the nanosize that achieve the finer dispersion of alumina nanoparticles in nanocomposites as compared to the direct mixing of nanoparticles. Two strategies were adapted to achieve the high flexural and impact properties (a) determining the optimum concentration of the alumina fillers at which the impact and flexural properties are highest, (b) preparation of hybrid composites at the optimum concentration of alumina fillers with the variation of weight percent of short fibers. The alumina nanoparticle and composites were characterized through the mechanical testing like, flexural testing, impact testing, thermogravimetric analysis (TGA), X-ray diffraction (XRD) and morphological observation by scanning electron microscope (SEM) analysis and optical microscope analysis.

Experimental

Materials and Preparation of Composites

Low viscosity multi-purpose epoxy resin specific gravity of 1.14 at room temperature, under the trade name of Bondtite PL-411 and the amine based hardener of specific gravity 0.98 of grade PH-861 supplied by Resinova Chemie Ltd. (India), was used as the base matrix material. The composition of the base matrix formulation was the mixture of 10-12 parts by weight of the hardener with the epoxy, which provide the pot life of 30 min at 40 ^{o}C. Micron sized alumina particles procured from the SASOL (Germany), was used as the filler material. PAN based carbon fiber supplied by the Zoltek (USA), and commercial grade E-glass fiber supplied by M/s Harsh Deep Industries (India), used as the reinforcing elements.

The epoxy resin was pre-heated using a heating plate up to 50 ^{o}C. The alumina nano particles and chopped glass/carbon fibers of length 1-7 mm (termed as short fibers) with the variation of 1, 2, 3, 4, and 5 wt% was considered for the open casting process. The respective particles and fibers were added separately into the resin in a 100 m*l* beaker with the aid of a mechanical stirrer running at 100 rpm for 4 h. To reduce the particle agglomeration by shear mixing process, the mixture was further homogenized at a relatively high stirring speed of 500 rpm for 30 min. For the hybrid composites; a constant amount of 2 wt% alumina particles were added to the fiber-matrix mixture. After being sealed in a glass beaker, it was transferred to bath ultrasonication (22 kHz in frequency, 55 % power intensity with a sweep mode) followed by probe ultrasonication for 30 min to achieve the fine particle or fiber dispersion and degassed for 4 h at 75 ^{o}C. The stoichiometric amount of hardener was added to the mixture after it had cooled down to ambient temperature. Hand stirring continued for the hardener homogenization throughout the whole mixture and subsequently placed in the vacuum oven to remove the air bubbles. The total material handling time was controlled for about 10-15 min. The processed mixture underwent solution casting at room temperature into the pre-designed strip-like mould cavities. Slurry samples were then carefully poured into the lightly lubricated metallic open mould leveled to the horizontal plane covered with aluminium foil from the bottom of the mould where as open top surfaces were exposed to atmosphere to facilitate the easy collapse of trapped air bubbles. The fabricated samples were cured at room temperature for 24 h in the air-circulating oven prior to demoulding, followed by post curing operation [27,28], to ensure that all the composites are perfectly cured before the impact and flexural test.

Characterization Techniques

Mechanical Test

The ASTM D6110-10 method was followed to prepare the test specimens for the impact energy test. Charpy test rig used for the investigations performed on an impact tester (CEAST) with pendulum energy of 11 J and a span of 60.0 mm. The tests were conducted at room temperature and normal atmospheric condition with the impact speed of the striking hammer was 3.46 m/s. Similarly, the defects free rectangular test coupons (ASTM D790-10), from each category, were tested for the measurement of flexural properties by using a three-point bending mode. The rig was mounted on an Zwick//Roell Z010 series universal testing machine at a crosshead speed of 1.27 mm/min at room temperature [24] with the span-to-depth ratio of 64 was maintained in order to ensure that the specimens failed due to flexural loading against the shear failure for small span-to-depth ratios. A minimum of five samples of each category was used for all the tests and the average value was considered for the analysis.

Micrograph Analysis for Fractured Test Specimens through SEM and Optical Microscopy

Surface morphology and the failure mechanism of fractured samples were examined at nano range through the high resolution scanning electron microscopy (HRSEM) equipment Zeiss (EVO MA 15), Germany, with the maximum vacuum capacity of 8.5×10^{-5} Torr. This equipment was capable of producing a magnification of 50,000× at 20 kV. The specimens

were glued to a metal base and coated with gold to prevent charge build-up by the electrons absorbed by the specimen. Micro-structural analysis was performed on both neat and nanophased particles/fiber reinforced epoxy composites. The structural deformation of the composite samples was avoided by submerging the samples in the liquid air. The voltage of 10 kV was maintained during the SEM operation. The Vaiseshika inverted metallurgical optical microscope-7001 IMS, India, with magnifying capacity of 25× to 1200× was used to capture the images under reflection mode.

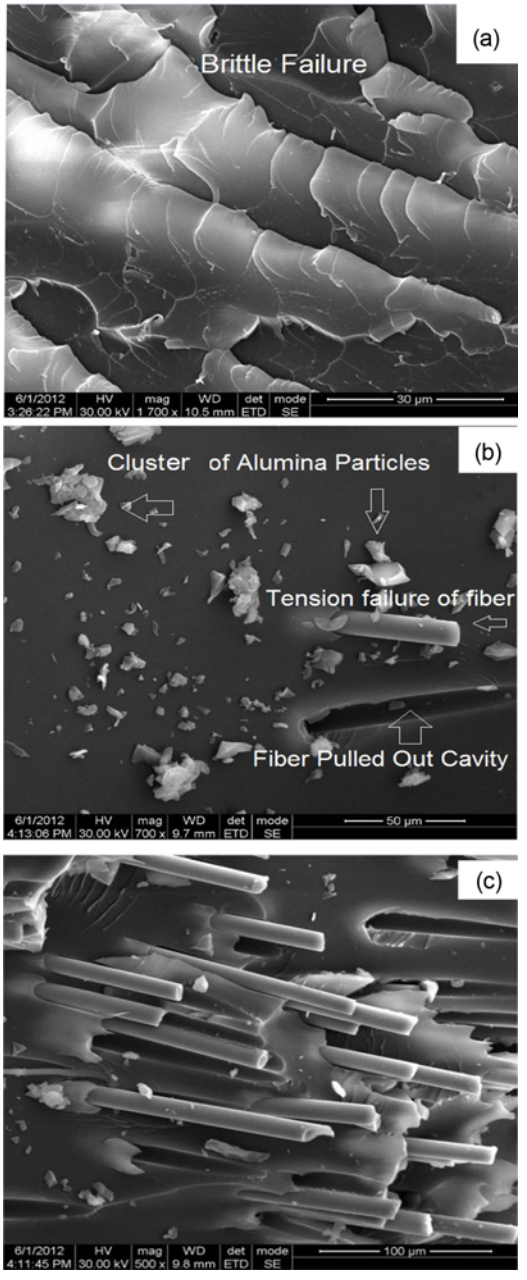

Figure 1. SEM photograph of fractured test specimen of (a) neat epoxy, (b) debonding of fiber, and (c) fiber fracture.

Results and Discussion

Epoxy/alumina Nanocomposite

SEM, TEM and XRD Analysis for Epoxy Nanocomposites

The fractography study of epoxy and hybrid composite was carried out through the SEM analysis. The Figure 1 shows the fractured pattern of neat epoxy and the hybrid composite test coupons after the impact tests. The Figure 1(a) shows the brittle fracture pattern of neat epoxy specimen where as the Figure 1(b) shows the fiber pull out and the fiber tension failure (Figure 1(c)) of the hybrid composites.

TEM was employed to investigate the reduction of micron size alumina into nanosize particles. Figure 2 shows the TEM micrograph of epoxy/alumina nanocomposites, which revealed that, the micron-sized as received alumina particles were converted into nano size. The size reduction of micron-sized alumina to nano size occurred due to the excessive compressive stress developed during the curing process. The uniform dispersion of alumina nanoparticle in epoxy matrix was achieved at low concentration, i.e., at 2 wt% (Figure 2(a)), while at higher concentration, i.e., 5 wt% of alumina particles in epoxy matrix (Figure 2(b)) shows the agglomeration of nanoparticles. Similar type of size transformation has been reported in literatures [28,29].

Figure 3 shows the XRD pattern of the as received alumina, epoxy and epoxy/alumina nanocomposites. XRD spectra of a micron size alumina show the characteristic peak at 14.5 °, 28.1 °, 38.3 °, 48.9 ° and 55.1 ° while epoxy

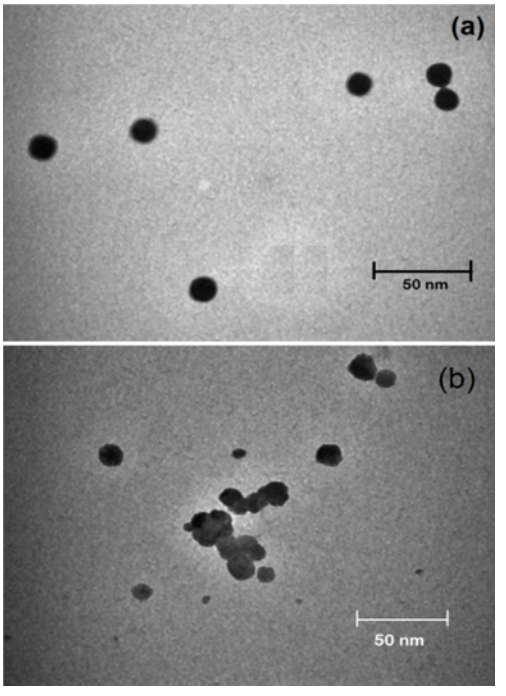

Figure 2. TEM image of epoxy composite containing alumina particles; (a) 2 wt% and (b) 5 wt%.

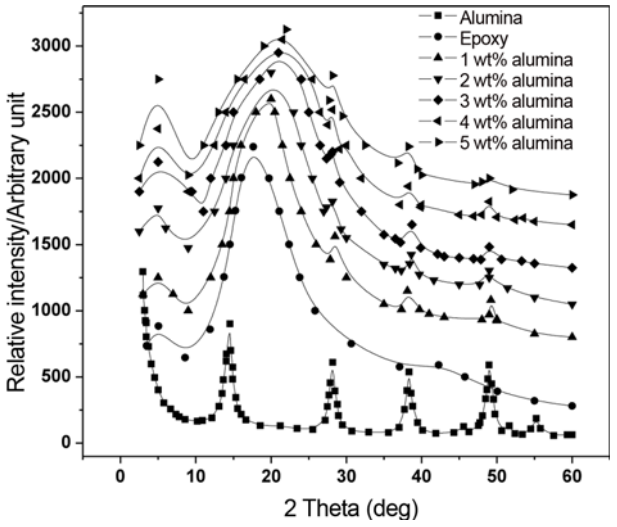

Figure 3. XRD patterns of alumina, epoxy and their samples from 0 wt%, 1 wt%, 2 wt%, 3 wt%, 4 wt% and 5 wt% alumina, scanned from 3 ^{o} to 60 ^{o} in 2θ scan [28].

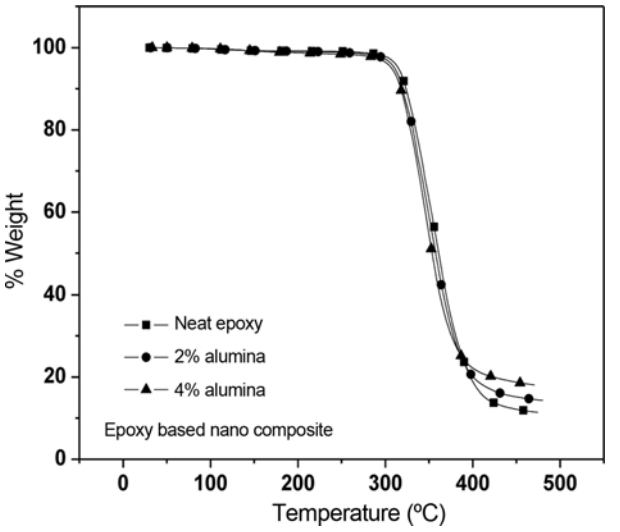

Figure 4. Thermogravimetric curve of neat epoxy with various alumina nano particles contents.

shows the characteristic peak at 5 ^{o} and 17.8 ^{o} respectively. However, XRD spectra of epoxy/alumina nanocomposites depict the characteristic peak of alumina at 28.1 ^{o}, 38.3 ^{o}, and 48.9 ^{o} respectively [30]. The intensities of diffraction peaks of alumina in epoxy/alumina nanocomposite decreases while the width of the peaks increases with an increase in wt% of alumina particle. It may be due to reduction of micron size alumina particles into nano size alumina particles during the curing operation. Similar result was observed in the case of micron size Al_2O_3 particle into nano size Al_2O_3 by reactive milling [31].

Thermogravimetric Analysis for Epoxy Nanocomposites

It is obvious that the dispersion of nanoparticles in the polymer matrix will significantly change the properties of nano composites [32,33]. Thermo gravimetric analysis (TGA) was carried out to understand the influence of the alumina nano particles on the thermal stability of the epoxy/ alumina nanocomposites. Figure 4 exhibits the TGA curves of the neat epoxy and epoxy/alumina nanocomposites under nitrogen atmosphere at a heating rate of 10 ^{o}C/min. All TG curves (Figure 4) present a C type thermal decomposition process [25], i.e. only one thermal decomposition step in the temperature range 30-475 ^{o}C. The decomposition region is centered between, 270-460 ^{o}C. It was observed that, an addition of up to 2 wt% of alumina nanoparticles results in a rightwards shift of TG curve of epoxy/alumina nanocomposites as compared to neat epoxy TG curve. Qi *et al.* [34] has been reported the similar rightwards shift of TG curve of epoxy based nanocomposites for various concentration of fillers. Further increase in the concentration of alumina nanoparticles in epoxy/alumina nanocomposites results in a leftward shift of TG curves. The rightward shift of TG curve of epoxy/ alumina nanocomposite depicts improved thermal stability, which may be due to the improved dispersion of alumina nanoparticles in nanocomposites, while the leftward shift of TG curve of epoxy/alumina nanocomposite depicts decreased thermal stability. This may be due to the aggregation of alumina nanoparticles in nanocomposites. 3 % thermal degradation of epoxy was observed at 2 wt% loading of alumina nanoparticles, and the TGA curve shifts rightward to 5 ^{o}C compared with neat epoxy, while for the loading of 4 wt% of alumina nanoparticles depicts TGA curve shift leftward to 8 ^{o}C.

Charpy Impact Test of Epoxy/alumina Nanocomposites

Charpy impact test was carried out at room temperature to understand the influence of alumina nano particles on the impact properties of epoxy/alumina nano composites. The impact energy (E) was calculated by using the equation (1)

$$E = \frac{\Delta E}{w \times t} \quad (1)$$

ΔE is the impact energy absorbed during the impact loading; w and t are the width at the notch point and thickness of specimen, respectively.

Figure 5 shows the effect of alumina nanoparticles on the Charpy impact energy of epoxy/alumina nanocomposites. With an increase in weight percentage of alumina nanoparticles in epoxy matrix, the impact energy increases up to a critical concentration and decreases thereafter. The impact energy of the alumina nano particle reinforced composite materials attains its optimum value at critical concentration of 2 wt%. The improvement in the impact energy was 84 % more than that of neat epoxy and reduced gradually thereafter. However, at 5 wt% loadings of alumina nano particles, a drastic reduction in the impact energy was observed, but a net gain of 44 % over the neat epoxy was recorded. Wetzel *et al*. [35] has been conducted a series of experiment to study the

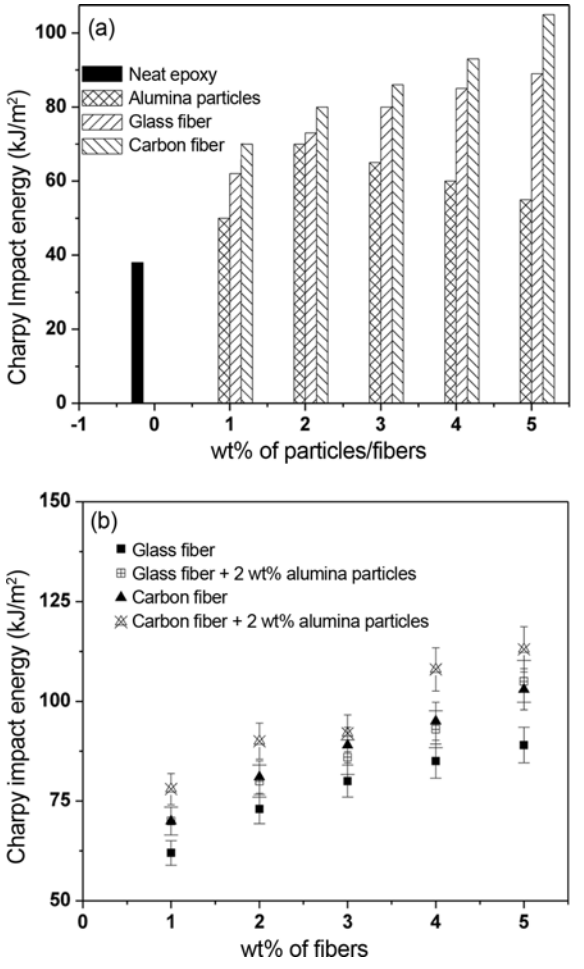

Figure 5. Effect of the (a) individual addition of the alumina particles, the glass/carbon fibers and (b) the addition of the glass/carbon fibers along with/without alumina particles over the range of weight fraction for the Charpy impact energy of epoxy based composites.

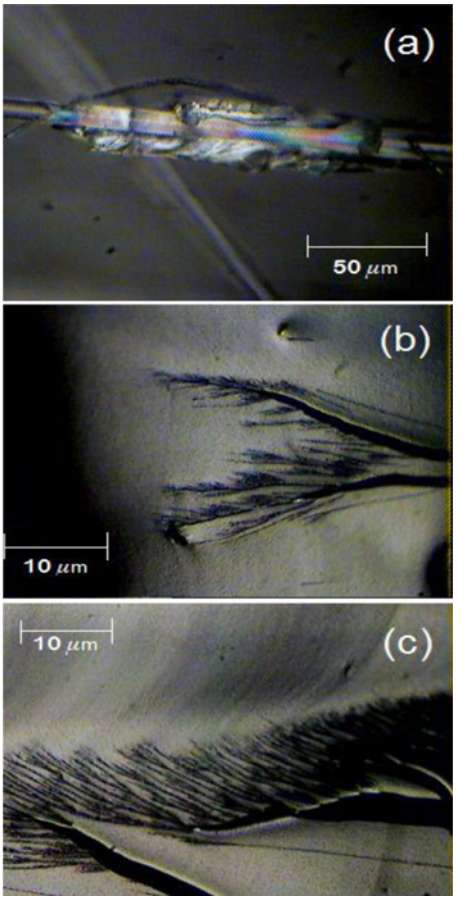

Figure 6. (a) Brittle failure of the matrix surrounds the fiber, and the fractured surface of alumina particles and the glass/carbon fiber reinforced composite materials (b), (c).

impact behavior of epoxy nanocomposites and strong improvement on the impact behavior of the composites was reported up to certain critical loading of alumina particles to the epoxy matrix. At higher filler volume contents, the impact energy decreases gradually. However, it remains well above the performance of the neat polymer. These results can be linked with the stress concentration effect. Wetzel *et al.* [35] had reported that, the nanoparticles induce several energies absorbing mechanisms in the matrix, which is the cause of the strong increase in impact energy correspond to lower vol.% of filler addition where as for the higher vol.% of filler addition, the particles agglomeration induce failure in the way large particles would do. However, the dramatic decrease in impact energy has been observed, which may be due to the geometrical properties of the particles, the inhomogeneous dispersion state, and energy dissipating fracture mechanisms [35].

The improvement in impact energy at lower concentrations of alumina nanoparticles is due to the better dispersion of nano sized alumina particles that possess greater interfacial areas in between the particle and matrix. This leads to the uniform coating of alumina particles by the epoxy resin. At higher concentration, the phenomenon of agglomeration leads to the drop in impact property of the nano composite, as aggregated alumina nano particles tend to initiate more defects like entrapment of tiny air pockets within the polymer matrix. Huang *et al.* [36] had reported the similar kind of effect for the epoxy/clay composites.

Flexural Test of Epoxy/alumina Nanocomposites

Three point flexural tests were carried out at room temperature to understand the resistance of the composite against the flexural loading over the range of particles and fiber loading in the epoxy matrix. The values of flexural strength σ_f and modulus, E_f were calculated according to the equations [2] and [3].

$$\sigma_f = \frac{3PL}{2bd^2}\left[1+6\left(\frac{D}{L}\right)^2-4\left(\frac{d}{L}\right)\left(\frac{D}{L}\right)\right] \quad (2)$$

And,

$$E_f = \frac{L^3}{4bd^3}\frac{\Delta P}{\Delta x} \quad (3)$$

here P is the maximum load (N), L is the span length (m), b is the specimen width (m), d is the specimen depth (m), D is the vertical deflection of the specimen centre line (m), and $\Delta P/\Delta x$ is the slope of the linear region of the force-displacement curve (Nm^{-1}).

Figure 7(a) shows the effect of alumina nanoparticles on the flexural strength of epoxy/alumina nanocomposites. With an increase in weight percentage of alumina nanoparticles in the epoxy matrix, the flexural strength increases up to a critical concentration and decreases thereafter in higher concentration of alumina nanoparticles in the epoxy matrix. It was observed that the flexural strength of the alumina particles loaded nano composites attained its optimum value (20 % more than neat epoxy) at a certain wt% (3 wt%) and gradually decreases thereafter for the high concentration of alumina particles. The improved flexural strength was due to the improved dispersion of alumina nanoparticle in the epoxy matrix while at higher concentration, aggregation of alumina naonoparticles reduces the flexural strength of the nanocomposites. The flexural modulus of epoxy/alumina nanocomposites also increases with the addition of alumina nanoparticles (Figure 7(b)). The net gain of 35 % over the neat epoxy is achieved corresponding to 5 wt% addition of alumina particles. It was observed that, at 2-3 wt% loading of alumina nanoparticles in the epoxy matrix, the maximum improvement in the flexural strength and impact energy for the composites was achieved. Thus, 2 wt% loading of alumina nanoparticles was selected as the optimum concentration for the preparation of hybrid glass/carbon fiber reinforced epoxy/alumina composites by varying the concentration of short glass/carbon fiber in the epoxy matrix. Xu *et al.* [37] had reported that, the flexural strength is increased due to the addition of 2 phr nanoclay into the epoxy matrix, whereas, adding more clay (4 phr) leads to a drop in flexural strength and mentioned that, this phenomenon might be resulted from the comparatively poorer dispersion of nanoclay and more possibility of the existence of voids in composites. Similarly Omrani *et al*. [38] had reported that, the flexural modulus was increased corresponding to the optimum loadings of 2 phr alumina nano particles and decreased for

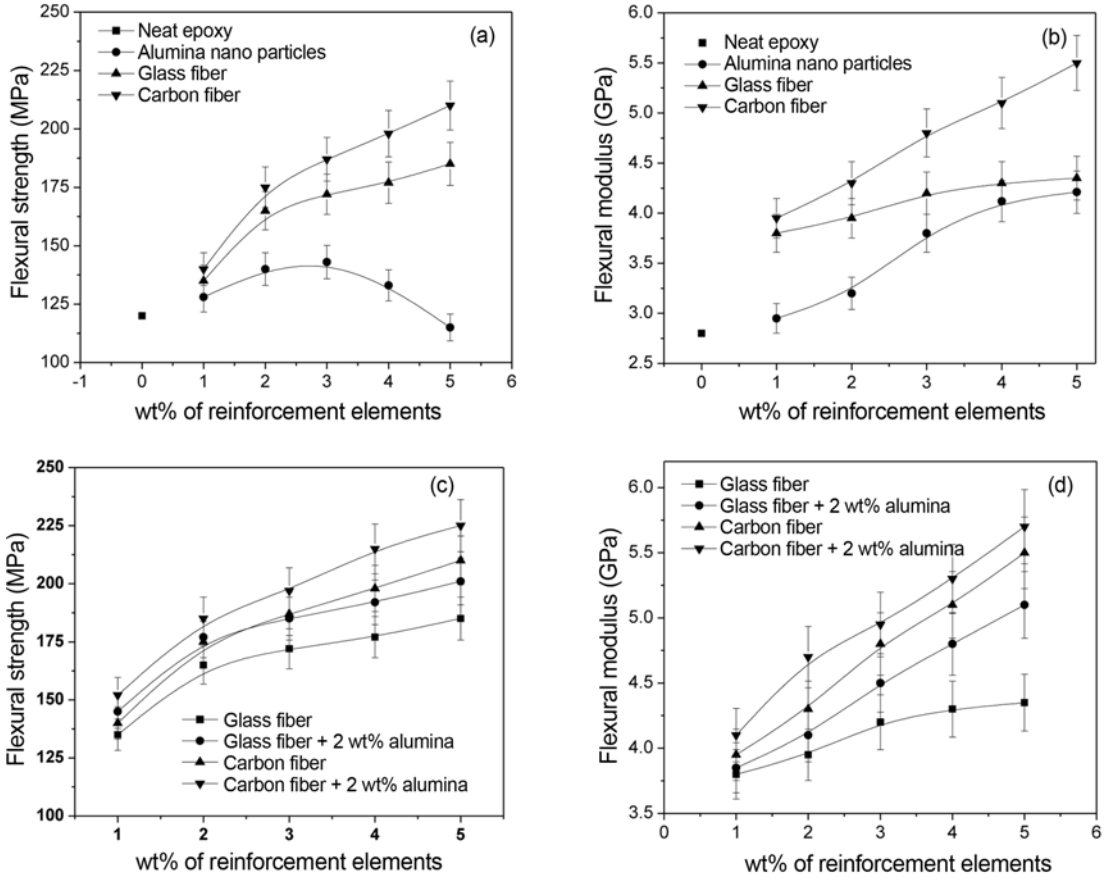

Figure 7. Effect of the individual addition of the alumina particles, the glass/carbon fibers (a), (b) and the addition of the glass/carbon fibers along with/without alumina particles (c), (d) over the range of weight fraction for the flexural strength and flexural modulus of epoxy based composites.

higher loadings of nano particles. This increase of property may be due to more effectively swell of the filler in the resin matrix leading to reliable dispersion and lager stiffness.

Glass/carbon Fiber Reinforced Epoxy/alumina Hybrid Composites

Charpy Impact Test of Hybrid Composites

Figure 5(b) shows the influence of variation of short glass/carbon fiber on the impact property of epoxy matrix. With the increase in fiber loadings resulted in an improvement in impact energy of the composites irrespective of the type of fibers. Net gain in impact energy of 135 % and 195 % was recorded as compared to neat epoxy for the addition of 5 wt% glass fiber and carbon fiber respectively. The response of carbon fiber loaded composite over the range of fiber addition shows superior impact properties over the glass fiber reinforced composites. The addition of fibers more than 5 wt%, seizes the flowability properties of the composites, thus the fiber loadings are limited to 5 wt% as the maximum fiber loading in the epoxy matrix. The tortuous fracture paths for glass fiber (Figure 6(b)) and carbon fiber (Figure 6(c)) reinforced hybrid composite confirms that a large amount of energy was absorbed in such types of composites. Qi *et al.* [34] had also reported the similar pattern for the impact fractured surfaces.

The impact properties of the fiber loaded composite materials were further enhanced due to the addition of the 2 wt% of alumina nanoparticles along with the short glass/carbon fibers into the epoxy matrix (Figure 5(b)). This may be due to the mechanism leading to the creation of the stronger interface that led to enhanced crack deflection, and micro-cracking (Figure 1(b), (c)), as a result, a further improvement in properties was observed. It is to be noted that, with the increase of the wt% of fiber resulted in the increase in the impact energy of the hybrid composite irrespective of the type of fiber addition. The optical micrograph of fractured test specimens of fiber reinforced composite (Figure 6(a)) shows the poor bonding of fiber with matrix at the interfacial region for the neat epoxy/fiber composites whereas the bonding strength was improved in the case of fiber and particle reinforced hybrid composite materials (Figure 6(b), (c)).

Flexural Test of Hybrid Composites

Figure 7(c), (d) shows the flexural behavior of alumina nanoparticles with randomly distributed short glass fibers and carbon fibers in epoxy based composites. The flexural strength of short glass fibers and carbon fibers loaded composite increases with the increase of the wt% of fibers contents. The net gain of 130 %, 170 % in the flexural strength (Figure 7(c)) and 55 %, 95 % in flexural modulus (Figure 7(d)) was recorded as compared to neat epoxy corresponding to the addition of 5 wt% glass fiber and carbon fiber respectively. Addition of alumina nanoparticles (2 wt%) along with the short glass fiber and carbon fiber in the epoxy matrix exhibits further improvement in flexural strength and flexural modulus in a steady manner over the range of fiber addition. The improvement in the properties observed to be 18 %, 26 % in the flexural strength and 65 %, 85 % in the flexural modulus as compared to the neat epoxy; whereas, 82 %, 105 % in flexural strength and 17 %, 5 % in flexural modulus as compared to 5 wt% concentration of its neat fiber reinforced composite materials. This improvement in properties is due to the improved dispersion and large interface areas of nano particles in contact with matrix material, which significantly improves the effective stress transfer from the matrix to particles. The surface of alumina nano particles led to increase in the effective interfaces surface for energy absorption. This creates a good interlocking mechanism with the surface of both fiber and matrix. Further, addition of alumina nanoparticle in the epoxy retains the low viscosity of the resin for prolonged periods and ensures the proper penetration of liquid resin into the fiber bundles.

Examinations on the fracture surfaces of particulate-filled epoxy resins visually by scanning electron microscope methods can often reflect detailed information on the cause and location of failure. Several mechanisms of crack propagation and failure were known to be applicable for filled epoxy resins. The cracks may pass through the particles if the fillers are weak, known as trans-particulate fracture, or they may pass around if the particles are strong enough. On the other hand, failure may occur by interfacial debonding or by cohesive failure of the matrix. Figure 1(a) shows a fracture surface for the neat epoxy matrix, which reveals a brittle behaviour characterized by large smooth areas and fracture steps in the direction of crack propagation. The crack usually initiates from surface defects or high stress regions. Figure 1(a) depicts the rough surface and shear cusps developed by nucleation and propagation of micro shear zones within the matrix ligament. This observation is consistent with the brittle failure mechanisms of epoxy materials as mentioned by the same authors [27]. In addition, Figure 1(b) clearly shows the pullout, detachment and debonding of some of the fiber which indicates the poor interfacial adhesion of the fiber with the epoxy matrix. The breaking of fiber could be due to the lack bonding strength at the vicinity of fiber/epoxy in the inner space of the fiber. Zhao *et al.* [39] have also emphasized on the improvement of toughness and ductility of the composites through the incorporation of nano particles into the epoxy matrix.

Conclusion

In the present study, the enhancements in the mechanical properties like impact and flexural properties of the neat epoxy was achieved due to the individual addition of alumina particles, short glass/carbon fibers into the epoxy matrix. The nano-scale size transformation of as received micron sized alumina particles to nano size within the epoxy

matrix was achieved during the curing process. The nano scale dispersion of alumina nanoparticles is achieved at an optimum concentration (2 wt%) of alumina nanoparticles. The higher concentration of alumina nanoparticles (5 wt%) results in an aggregation of alumina nanoparticles in the epoxy matrix. The addition of alumina nanoparticles into the epoxy matrix also results in the improvement of the thermal stability of the epoxy/alumina nanocomposites.

Furthermore, the addition of optimum concentration (2 wt%) of alumina nanoparticles into the short glass/carbon fiber reinforced epoxy composites result in an improved impact strength, flexural modulus and flexural strength as compared to neat epoxy and fiber reinforced epoxy composites. The improvement was due to the better stress transfer properties from fiber and nanoparticles to the matrix, due to the existence of strong interfacial interactions between both reinforcement and matrix, which depict the higher resistance to fiber pullout as compare to fiber reinforced composites without alumina nanoparticles.

Acknowledgements

The first author would like to thank the Dept. of Mechanical Engineering, IIT (BHU), Varanasi, India, for providing the necessary experimental facilities and technical support to carry out this research works.

References

1. B. Wetzel, F. Haupert, and M. Q. Zhang, *Compos. Sci. Technol.*, **63**, 2055 (2003).
2. D. Bachtiar, S. M. Sapuan, A. Khalina, E. S. Zainudin, and K. Z. M. Dahlan, *Fiber. Polym*., **13**, 894 (2012).
3. S. P. Rwei, C. Y. Cheng, G. S. Liou, and K. C. Cheng, *Polym. Eng. Sci.*, **45**, 478 (2005).
4. J. F. Coulon and H. Maillard, *Eur. Phys. J. Appl. Phys*., **49**, 1 (2010).
5. C. S. Wang and M. C. Lee, *Polymer*, **41**, 3631 (2000).
6. D. Kim, I. Chung, and G. Kim, *Fiber. Polym*., **14**, 2141 (2013).
7. S. R. Reid and G. Zhou, "Impact Behaviour of Fibre-reinforced Composite Materials and Structures", 1st ed., Woodhead Publishing Limited, Loughborough, United Kingdom, 2000.
8. S. Sanchez-Saez, E. Barbero, R. Zaera, and C. Navarro, *Compos. Sci. Technol*., **65**, 1911 (2005).
9. V. J. Hawyes, P. T. Curtis, and C. Soutis, *Compos. Pt. A-Appl. Sci. Manuf.*, **32**, 1263 (2001).
10. E. V. Morozov, K. E. Morozov, and V. Selvarajalu, *Compos. Struct.*, **62**, 361 (2003).
11. S. Zhao, L. S. Schadler, H. Hillborg, and T. Auletta, *Compos. Sci. Technol*., **68**, 2976 (2008).
12. S. Deng, L. Ye, and K. Friedrich, *J. Mat. Sci.*, **42**, 2766 (2007).
13. M. Q. Zhang, M. Z. Rong, S. L. Yu, B. Wetzel, and K. Friedrich, *Wear*, **253**, 1086 (2002).
14. A. Yasmin, J. J. Luo, J. L. Abot, and I. M. Daniel, *Compos. Sci. Technol*., **66**, 2415 (2006).
15. C. Lam, K. Lau, H. Cheung, and H. Ling, *Mater. Lett*., **59**, 1369 (2005).
16. A. Yasmin, J. L. Abot, and I. M. Daniel, *Scr. Mat*., **49**, 81 (2003).
17. H.-J. Song and Z.-Z. Zhang, *Tribo. Int*., **41**, 396 (2008).
18. P. N. B. Reis, J. A. M. Ferreira, Z. Y. Zhang, T. Benameur, and M. O. W. Richardson, *Compos. Pt. B-Eng.*, **46**, 7 (2013).
19. Y. H. Liao, O. Marietta-Tondin, Z. Liang, C. Zhang, and B. Wang, *Mater. Sci. Eng. A*, **385**, 175 (2004).
20. Y. Xu and S. V. Ho, *Compos. Sci. Technol*., **68**, 854 (2008).
21. A. A. Azeez, K. Y. Rhee, S. J. Park, and D. Hui, *Compos. Pt. B-Eng.*, **45**, 308 (2013).
22. H. Alamri, I. M. Low, and Z. Alothman, *Compos. Pt. B-Eng.*, **43**, 2762 (2012).
23. M. Moniruzzaman, F. Du, N. Romero, and K. I. Winey, *Polymer*, **47**, 293 (2006).
24. Y. Dong, D. Chaudhary, C. Ploumis, and K. T. Lau, *Compos. Pt. A-Appl. Sci. Manuf.*, **42**, 1483 (2011).
25. V. Kostopoulos, A. Baltopoulos, P. Karapappas, A. Vavouliotis, and A. Paipetis, *Compos. Sci. Technol*., **70**, 553 (2010).
26. A. F. Avila, M. I. Soares, and A. S. Neto, *Int. J. Impact. Eng*., **34**, 28 (2007).
27. A . Mohanty and V. K. Srivastava, *Int. J. Sci. Eng. Res*., **3**, 1 (2012).
28. A. Mohanty and V. K. Srivastava, *Mater. Des*., **47**, 711 (2013).
29. A. Mohanty, V. K. Srivastava, and P. U. Sastry, *J. Appl. Polym. Sci.,* **131**, 1 (2014).
30. B. Akbari and R. Bagheri, *Eur. Polym. J*., **43**, 782 (2007).
31. A. Rabiezadeh, A. M. Hadian, and A. Ataie, *Int. J. Ref. Met. Haz. Mat*., **31** 121 (2012).
32. P. B. Tambe, A. R. Bhattacharyya, S. Kamath, A. R. Kulkarni, T. V. Sreekumar, A. Srivastav, K. U. B. Rao, Y. Liu, and S. Kumar, *Polym. Eng. Sci*., **52**, 1183 (2012).
33. P. B. Tambe, A. R. Bhattacharyya, and A. R. Kulkarni, *J. Appl. Polym. Sci*., **127**, 1017 (2013).
34. B. Qi, Z. Yuan, S. Lu, K. Liu, S. Li, L. Yang, and J. Yu, *Fiber. Polym*., **15**, 326 (2014).
35. B. Wetzel, F. Haupert, K. Friedrich, M. Q. Zhang, and M. Z. Rong, *Polym. Eng. Sci.*, **42**, 1919 (2002).
36. H. Huang and R. Talreja, *Compos. Sci. Technol*., **65**, 1964 (2005).
37. Y. Xu and S. V. Hoa, *Compos. Sci. Technol*., **68**, 854 (2008).
38. A. Omrani, L. C. Simon, and A. A. Rostami, *Mater. Chem. Phys.,* **114**, 145 (2009)
39. S. Zhao, L. S. Schadler, R. Duncan, H. Hillborg, and T. Auletta, *Compos. Sci. Technol.*, **68**, 2965 (2008).